Published in final edited form as:
Cell Cycle. 2007 April 15; 6(8): 972–981.

Identification of Primary Transcriptional Regulation of Cell Cycle-Regulated Genes upon DNA Damage

Tong Zhou[1], **Jeff Chou**[2], **Thomas E. Mullen**[1], **Rani Elkon**[3], **Yingchun Zhou**[1], **Dennis A. Simpson**[1], **Pierre R. Bushel**[2], **Richard S. Paules**[2], **Edward K. Lobenhofer**[4], **Patrick Hurban**[4], and **William K. Kaufmann**[1,*]

1 *Department of Pathology and Laboratory Medicine; Center for Environmental Health and Susceptibility, and Lineberger Comprehensive Cancer Center; University of North Carolina at Chapel Hill; Chapel Hill, North Carolina USA*

2 *Department of Health and Human Services; National Institute of Environmental Health Sciences; Research Triangle Park, North Carolina USA*

3 *Department of Human Genetics; Sackler School of Medicine; Tel Aviv University, Tel Aviv, Israel*

4 *Cogenics, a Division of Clinical Data; Morrisville, North Carolina USA*

Abstract

The changes in global gene expression in response to DNA damage may derive from either direct induction or repression by transcriptional regulation or indirectly by synchronization of cells to specific cell cycle phases, such as G1 or G2. We developed a model that successfully estimated the expression levels of >400 cell cycle-regulated genes in normal human fibroblasts based on the proportions of cells in each phase of the cell cycle. By isolating effects on the gene expression associated with the cell cycle phase redistribution after genotoxin treatment, the direct transcriptional target genes were distinguished from genes for which expression changed secondary to cell synchronization. Application of this model to ionizing radiation (IR)-treated normal human fibroblasts identified 150 of 406 cycle-regulated genes as putative direct transcriptional targets of IR-induced DNA damage. Changes in expression of these genes after IR treatment derived from both direct transcriptional regulation and cell cycle synchronization.

Keywords

microarray; cell cycle; ionizing radiation; human fibroblasts; EPIG

INTRODUCTION

Cell proliferation is a fundamental biological activity that is regulated through many gene products, including cyclin-dependent kinases (CDKs), enzymes for DNA replication and repair, enzymes for chromatin condensation and segregation, proto-oncogenes, and tumor suppressor genes.[1,2] Many cell cycle regulators undergo dramatic changes in levels of expression and activity to propel or regulate progression through the cell division cycle.[3] Identification of cell cycle-regulated genes will facilitate understanding of not only normal

*Correspondence to: William K. Kaufmann, PhD; Department of Pathology and Laboratory Medicine, Lineberger Comprehensive Cancer Center; University of North Carolina at Chapel Hill; Chapel Hill, North Carolina 27599 USA; Tel.: 919.966.8209; Fax: 919.966.3015; Email: wkarlk@med.unc.edu.

Previously published online as a *Cell Cycle* E-publication: http://www.landesbioscience.com/journals/cc/abstract.php?id=4106

biological processes during cell division but also mechanisms of pathologic response to environmental toxicants.

Microarray technology enables researchers to determine changes in expression of thousands of genes in cells and tissues in response to treatment with exogenous chemicals or drugs.[4,5] A commonly addressed question in microarray experiments is which genes are direct transcriptional targets of carcinogen-induced DNA damage, and which are altered secondarily to inhibition of cell cycle progression following DNA damage? It is not uncommon for hundreds or even thousands of genes to be changed significantly after a specific drug or toxicant treatment. However, toxic agents that cause DNA damage, such as IR, UV and chemotherapeutic drugs for cancer, usually inhibit cell proliferation by activating cell cycle checkpoint functions and causing growth arrest at specific cell cycle phases.[2,6,7] The synchronizing effect of the cell cycle checkpoint response to DNA damage can affect the expression of cell cycle- or growth-regulated genes at later times[8,9] masking direct transcriptional targets.

To quantify the effects on gene expression resulting from changes in the proportions of cells in G_1, S, G_2 and M phases of the cell division cycle, a baseline level for all transcripts in each of these phases must first be established, and then gene expression in a population of cells can be estimated when the proportionate distribution of cells in the various cycle compartments is known. Although global transcriptional regulation during the cell cycle has been widely investigated in many organisms using microarray technology,[1,3,10–15] none of the current methods used to synchronize cells results in 100% of the cells in a specific cell cycle phase. Furthermore, the cells become asynchronous with time after release from the synchronizing block. Therefore, the measured transcript levels do not truly represent a pure cell population.

In the present study, a model was developed to determine “true” expression levels of genes in each pure cell cycle phase. Cell-cycle-specific gene expression patterns and cell cycle-regulated genes were further identified by EPIG method.[16] Once the levels of cell cycle-regulated genes in pure G_1, S, G_2 or M phase cells were obtained, we were able to isolate effects of DNA damage-induced redistribution of cell cycle phases on expression of cell cycle-regulated genes, and then to identify direct transcriptional targets of a genotoxin.

MATERIALS AND METHODS

Cell lines and culture

Normal human fibroblasts, NHF1, NHF3 and NHF10, were derived from neonatal foreskins and established in culture according to established methods.[17] Immortalized cell lines were obtained by ectopic expression of human telomerase (hTERT), as previously described.[18,19] Fibroblasts were cultured in DMEM high-glucose medium (Invitrogen, Carlsbad, CA USA) supplemented with 2 mM L-glutamine (Invitrogen, Carlsbad, CA, USA) and 10% fetal bovine serum (FBS, Sigma Chemical Co, St. Louis, MO, USA). All cell lines were maintained at 37° C in a humidified atmosphere of 5% CO_2 and were routinely tested and shown to be free of mycoplasma contamination using a commercial kit (Gen-Probe, San Diego, CA, USA).

Cell irradiation

Cells were exposed to ionizing radiation in their culture medium, using a ^{137}Cs source (Gammacell of Canada) at a dose rate of 0.84 Gy/min. Sham-treated controls were subjected to the same movements in and out of incubators as irradiated cells.

Cell cycle compartment determination

For quantification of G_1, S and G_2 phase cells, 10 μM 5′-bromo-2′-deoxyuridine (BrdU, Sigma Chemical Co.) was added to culture medium at various times after irradiation to label S phase cell DNA and cultures were incubated for another 2 hours. Cells were harvested, washed with phosphate-buffered saline (PBS), and fixed with 67% ethanol in PBS. Cells were stained with fluorescein isothiocyanate (FITC)-conjugated anti-BrdU antibody (BD Biosciences, San Jose, CA, USA) and propidium iodide (PI, Sigma Chemical Co., St. Louis, MO, USA), then G_1, S and G_2 phase cells were enumerated by flow cytometry as previously described.[20–22] For analysis of M phase cells, cells were harvested at various times after irradiation, washed with PBS, fixed in 1% formaldehyde in PBS for 30 min, and then fixed in 67% ethanol in PBS. Cells were incubated in 0.5 μg/100μl anti-phospho-histone H3 antibody (Upstate Biotechnology Inc., Lake Placid, NY, USA) for 2 h, and then stained with FITC-conjugated anti-rabbit antibody (Santa Cruz) and propidium iodide.[23–25] Flow cytometric analyses to enumerate mitotic cells were done using a FACScan flow cytometer and Summit software (DakoCytomation, Fort Collins, CO, USA).

Cell synchronization

NHF1, NHF3 and NHF10 cells were synchronized as previously described.[19,26,27] Briefly, cells were plated at a density of $1.3 \times 10^4/cm^2$ and allowed to grow for 8 days to confluence-arrest in G_0 phase. During this time cell growth medium was changed on days 3 and 5 post-seeding. Arrested cells were released from dishes with trypsin, reseeded at $1.3 \times 10^4/cm^2$ and then incubated for 8 h to allow them to reach mid G_1. Cells similarly released from G_0 were incubated with the DNA polymerase inhibitor, aphidicolin (APC), at a concentration of 2 μg/ml for 24 h to collect cells at the beginning of S. APC was washed out and cells incubated for 3 hr to allow accumulation to mid S phase. Cells that were released from APC treatment also were incubated for 8 h to accumulate in G_2. Colcemid at 100 ng/ml was added to such G_2 cells and cells were incubated an additional 4 h to collect cells in mitosis (M). Ten million cells were harvested at each cell cycle phase for RNA isolation. Two million cells were sampled for flow cytometric analysis of DNA content by staining with propidium iodide. Modfit commercial software (Verity Software House Inc.,Topsham, ME, USA) was used to determine the proportions of cells in G_0/G_1, S and G_2/M. The proportions of cells in M were determined by flow cytometric enumeration of phospho-histone H3-expressing cells with 4N DNA content.

Oligo DNA microarray

Total RNA was isolated from synchronized cell populations using a Qiagen RNeasy kit. The quality of all RNA samples was confirmed using an Agilent 2100 Bioanalyzer. Microarray analysis was then performed through a contract with Icoria Corporation as follows. Briefly, 1 μg of sample RNA and global reference RNA (Stratagene, La Jolla, CA, USA) were converted to cDNA with reverse transcriptase then amplified using T7 RNA polymerase while labeling with either Cy3-dUTP or Cy5-dUTP (Agilent's Low RNA Input Linear Amplification Kit, Agilent Techologies, USA). The quality of each labeled cRNA was evaluated using an Agilent 2100 Bioanalyzer prior to hybridization. 750 ng of Cy3 and Cy5-labeled cRNA were used in the hybridization. The labeled cRNA from samples was hybridized with the labeled global reference cRNA on an Agilent 22k human 1A array (Agilent Techologies, USA) in a hybridization oven (Robbins Scientific Model 400, 1040-60-1AG, Sunnyvale, CA, USA) at 60°C for 17 h. Hybridization of sample RNA against reference RNA was done twice with a fluorophore reversal (dye swap). Following hybridization, the arrays were scanned using the Agilent DNA Microarray Scanner with SureScan® Technology and microarray images were analyzed using Agilent Feature Extraction Software (v7.1).

Computational analysis of microarray data

(1) Cell cycle-regulated gene extraction. As previously reported[26] and shown in (Table 1), the synchronization methods yielded populations of cells that were highly enriched in selected cycle-phase compartments but the synchronization was imperfect. Cultures synchronized in G_1 phase displayed 82–91% 2N DNA content with small proportions of cells in S, G_2 and M. Cultures that were synchronized to S, G_2 and M displayed 46–71%, 54–70% and 23–32% of cells in these phases, respectively. Global gene expression profiles were generated from the synchronized cell populations. To calculate theoretically "pure" G_1-, S-, G_2- or M-specific gene expression levels, four simultaneous equations were derived for each gene based on the microarray-determined expression levels and the proportions of cells in each cycle phase for each of the synchronized samples. The expression levels of a gene in G_1, S, G_2, or M, assuming that it has a linear relationship with the proportion of cells in each cycle compartment, may be expressed as:

$$gene_{i,G1} = f_{G1,G1} \times GENE_{i,G1} + f_{S,G1} \times GENE_{i,s} + f_{G2,G1} \times GENE_{i,G2} + f_{M,G1} \times GENE_{i,M}$$
$$gene_{i,G2} = f_{G1,G2} \times GENE_{i,G1} + f_{S,G2} \times GENE_{i,s} + f_{G2,G2} \times GENE_{i,G2} + f_{M,G2} \times GENE_{i,M}$$
$$gene_{i,S} = f_{G1,S} \times GENE_{i,G1} + f_{S,S} \times GENE_{i,S} + f_{G2,S} \times GENE_{i,G2} + f_{M,S} \times GENE_{i,M}$$
$$gene_{i,M} = f_{G1,M} \times GENE_{i,G1} + f_{S,M} \times GENE_{i,S} + f_{G2,M} \times GENE_{i,G2} + f_{M,M} \times GENE_{i,M}$$

where $gene_{i,j}$ is the measured expression level of gene i in cultures synchronized in phase j that is an average of the duplicate arrays (C3 or C5 labeling), $j \in \{G_1,G_2,S,M\} \cdot f_{j,G1}$, is the fraction of G_1 cells in cultures synchronized in phase j ; conversely for $f_{j,S}$, $f_{j,G2}$ and $f_{j,M} \cdot GENE_{i,j}$ is the expression level of gene i if the gene was expressed in a perfectly synchronized phase j. The equations were simultaneously solved to calculate "pure" G_1-, S-, G_2- and M-specific expression levels. In this model, interactions between genes or cell cycle compartments were assumed to have no effect on the equations.

A targeted evaluation of 45 well-known cell cycle-regulated genes demonstrated that the model expanded the range of variation in expression levels across the cell cycle. The levels of transcripts specific to M cells were most impacted by the model (Table 2). This was to be expected as synchronization yielded an M population representing only 22–32% of the cells, while the model estimated transcript levels for a theoretically pure sample of mitotic cells.

$GENE_{i,j}$, expression level of a gene with purity correction, was applied in EPIG analysis for extraction of patterns of cell cycle-regulated gene expression patterns and significant genes. In the EPIG method, the extracted log2 pixel intensity ratio values (sample vs. reference) were preprocessed, which included systematic variation normalization, dye-swap correction, and cell line alignment.[28] Three parameters, the correlation coefficient within a specific pattern, the magnitude of change, and the signal-to-noise ratio (SNR), were employed for selection of significant genes.[16]

(2) Identification of primary transcriptional targets. Gene expression in sham- or IR-treated cell populations was estimated using $GENE_{i,j}$ weighted by the proportions of cells in G_1, S, G_2 and M. The estimated values were then compared with the observed values from microarrays to distinguish changes in gene expression caused by alterations in cell cycle distribution from changes caused directly by IR treatment. The comparisons were done by paired t-test to identify significant genes showing difference between the estimated values and the observed values.

(3) Gene ontology analysis of significant genes. Categories of genes that were over-represented in a selected gene list compared to what was represented in the microarray were analyzed using

EASE (http://apps1.niaid.nih.gov/david/). Such over-represented categories represent biological "themes" of a given list.

(4) Identification of transcription factors (TFs) in cell cycle-regulated genes. Computational promoter analysis was done using the PRIMA software, described in detail by Elkon et al.[29] Briefly, given a target set and a background set of promoters, PRIMA performs statistical tests, based on hypergeometric distribution, aimed at identifying TFs whose binding site signatures are significantly more prevalent in the target set than in the background set. In this study, each of the two sets of cell cycle-regulated genes (IR-target genes and non-IR-target genes) was considered a target set and the entire set of genes represented on the microarray served as the background set. PRIMA uses position weight matrices (PWMs) as models for regulatory sites that are bound by TFs. PWMs that represent human or mouse TF binding sites were obtained from the TRANSFAC database.[30] Putative promoter sequences corresponding to all known human genes were extracted from the human genome, masking out repetitive elements (Ensembl, version 27).[31] PRIMA promoters' scan was done on both strands and was confined to the region from 600 bp upstream to 100 bp downstream to the putative genes' transcription start site.

RESULTS

Extraction of cell cycle-regulated genes

From the purity-corrected microarray data, EPIG was able to identify nine cell cycle-specific expression patterns (Fig. 1) and 2410 genes or ESTs as cell-cycle-specific based on criteria of three parameters: correlation coefficient within a specific pattern ($r \geq 0.64$, $n = 24$, $p < 1\times10^{-6}$), the magnitude of change (log2 ratio of sample vs. reference > 0.4), and the signal-to-noise ratio (SNR > 3, $p < 0.01$) (Chou, Zhou, Bushel, Kaufmann and Paules, in preparation). The number of genes in each pattern ranged from 19 to 473 (Table 3). All expected patterns of gene expression across the cell cycle were detected. About 500 genes were expressed at highest levels in G_1 and at lower levels in S, G_2 and M (Patterns 1 and 2). Over 1100 genes were expressed at highest levels in S and at variably lower levels in G_1, G_2 and M (Patterns 3–7). No pattern displayed a peak of gene expression in G_2 but over 700 genes in Patterns 8 and 9 displayed maximal expression in M. Among the genes that were expressed at highest levels in G_1 were the well-known growth-enhancing transcription factor *Myc*, and *GOS2*, a gene known to be expressed highly in G_1 cells and to regulate the G_0 to G_1 transition.[32] Among the genes expressed at highest levels in S were many whose protein products are known to be required for DNA replication such as *ORC3*, *ORC4*, *ORC6*, *CDC45L*, *CDC6*, *CDC7L*, *MCM2*, *MCM3*, *MCM6*, *MCM7*, *POLA2*, *PCNA*, *RFC2*, *RFC3*, and *RFC5*. In patterns 8 and 9 with highest expression in M were *BUB1B*, *CCNB1*, *CDC20*, *CDC25C* and *PLK* that are known to regulate cell progression through G_2 and M. Thus, many genes that displayed cell-cycle-specific gene expression encode proteins that are expected to function during the phases of maximal expression.

However, cycle-specific changes in gene expression in synchronized cell populations may not reflect the changes that occur in physiologically cycling cell populations. Some genes selected by above method, although showing pattern-specific expression, may not be truly cell-cycle-regulated genes. Changes in these genes might simply reflect the G_0/G_1 transition (highest expression in G_1), a response to aphidicolin (highest expression in S), or a response to colcemid (highest expression in M). For those truly cell-cycle-regulated genes, changes in expression levels should reflect alterations in proportions in each phase of the cell cycle.

To further test the truly cell cycle-regulated genes, a second experiment was performed in which NHF1 cells were cultured and harvested at seven different times between days 2 to 3 after reseeding. These cultures contained different proportions of cells in each cycle-phase

(Table 4) and gene expression levels were determined for each culture by microarray. The hypothesis for this experiment was that expression levels of cell cycle-regulated genes were linearly correlated with the proportions of cells in each cycle phase and variations in these proportions in normally cycling cell population would alter the levels of expression of cell cycle-regulated genes (given that expression levels of a cell cycle-regulated gene in each pure cell cycle phase are stable and known). Based on the measured proportions of cells in each cycle phase in each culture, the expression levels of the 2410 cell cycle-specific genes identified earlier were estimated to compare with the microarray-determined expression levels. A gene was identified as cell-cycle-regulated only when its expression level was well-estimated ($r > 0.75$, $P < 0.05$) by the proportions of cells in the various cycle phases. A total of 406 genes were confirmed as cell cycle-regulated by displaying a significant high correlation between the estimated and the microarray-determined expression levels. GO analysis of the 406 genes showed that all cell-cycle-related categories were significantly over-represented. The same analysis applied to the remainder of the 2410 genes yielded 12 categories related to intracellular processes, nucleotide and nucleic acid metabolism, and RNA binding, but no cell cycle-related categories.

Identification of transcriptional targets of ionizing radiation

NHF1, NFH3 and NHF10 human fibroblast lines in logarithmic growth were treated with 1.5 Gy IR, a dose that inhibited colony formation by 40–45%. Cells were harvested at 2, 6 and 24 h post-IR for microarray analysis of gene expression. Quantitative analysis of cell cycle compartments after IR treatment indicated that the proportions of G_1, S, G_2 and M cells changed markedly, especially at 24 h when the G_1 population was substantially enriched and the S and M compartments were severely depleted (Table 5, Fig. 2). These changes in the distribution of cells across the cell cycle were primarily the consequence of the p53-dependent G_1 checkpoint response.[33] The cell-synchronizing effects of IR leading to redistribution of cell cycle compartments were expected to affect the expression profiles of all 406 cell cycle-regulated genes.

According to the determined proportions of cells in each of the cycle compartments in sham- and IR-treated cells (Table 5) and the expression levels of the 406 genes in each presumed pure cell cycle phase, expression levels of these cell cycle-regulated genes were estimated. Changes in expression levels (log2 ratios of sample vs reference) of the 406 genes at 2, 6 and 24 h after IR-irradiation relative to sham-treated controls were obtained by subtracting expression level of sham-treated samples from IR-treated samples and the estimated values and the measured values were compared (Table 9, Supplement).

If the values were equivalent, it would suggest that changes in the expression levels of cell-cycle-regulated genes were associated with the IR-induced cell synchronization. A total of 193 genes with changes in expression levels showing no significant difference between the estimated values and the measured values were identified as non-targets of IR.

Alternatively, if changes in the expression levels of cell-cycle-regulated genes were associated with IR directly affecting transcription in addition to cell synchronization, the measured expression levels would be impacted by both of these effects, and the measured and estimated values would be different. Accordingly, 150 genes with measured transcript levels different than estimated values were identified as IR-target genes based on a statistical significance criterion (paired t-test, $P < 0.05$) and fold change threshold (log2 ratios of sample vs reference >0.4). These 150 genes represent putative direct transcriptional targets of IR, of which 134 were repressed and 16 were induced. Most of the IR-target genes (131) were recognized at 24 hr post-treatment, with 44 targets recognized at 6 hr and 3 targets recognized at 2 hr.

Gene ontology analysis of the 150 target genes yielded over-represented categories related to cell cycle, cell proliferation, DNA metabolism and DNA repair. Some well-known genes were *BUB1*, *CCNB1*, *CCNB2*, *CDC2*, *CDC20*, *E2F1*, *KNSL1*, *KNSL7*, *MCM2*, *MCM5*, *MCM7*, *PCNA*, *POLD1*, *RFC4*, *RFC5*, *TIMELESS*, *TOP2A*, *FANCA*, *RAD18*, and *RAD51* (Figs. 3a–c). Among the 193 non-target genes, *CCNE1*, *CDC45L*, *CDC6*, *CDKN2D*, *CENPE*, *CHEK1*, *LIG1*, *MSH2*, *ORC6L*, *POLA2*, and *POLE* were included (Fig. 3d) and over-represented categories from gene ontology also included biological process related to cell cycle, cell proliferation, DNA metabolism (Table 6). The 63 genes showing significant differences between observed and predicted but with fold changes less than 0.4 need be confirmed in further experiments.

Transcription factors involved in target and non-target cell cycle-regulated genes

Analysis of transcription factor binding sites in the promoters of the target and non-target cell-cycle-regulated genes showed that two factors, E2F and NF-Y, were enriched in both groups while cell cycle-dependent element (CDE) was significantly enriched in the target group and upstream stimulating factor (USF) was significantly enriched in the non-target group (Table 7).

DISCUSSION

Cell synchronization helps identify phase-specific genes[3,12,15] but does not provide quantitatively accurate expression levels of cell cycle-specific genes because of the lack of perfect synchrony. By applying simultaneous equations, the expression levels of genes in theoretically pure G_1, S, G_2 or M cell cycle phases were estimated. These gene expression levels were thereafter used to identify cell cycle-specific genes and to estimate the expression levels of cell cycle-regulated genes in an asynchronous cell population based on the proportions of G_1, S, G_2 and M cells. The results provide another image of the regulation of gene expression as human cells synchronously pass through the cell division cycle, and suggest that many cell cycle-regulated genes are actively repressed in response to IR-induced DNA damage.

It must be noted that artificially synchronized cell cycle phases do not biologically equal the phases existing in physiologically cycling cells. Although a total of 2410 genes or ESTs showing cell cycle-specific expression were identified based on nine extracted patterns by using EPIG method, they were not necessarily cycle-regulated genes. Many of these genes may have been selected because of serum stimulation after release from G_0 into G_1,[12] or by a direct response to aphidicolin or colcemid treatment.[27] Only genes whose expression levels could be correctly estimated in asynchronous cell populations based on the proportions of cells in the cycle compartments were accepted as cell cycle-regulated. A total of 406 among the 2410 genes were identified as cell cycle-regulated genes.

One of the purposes of the present study was to identify the transcriptional targets of a genotoxin among the cell cycle-regulated genes. It has been well-documented that IR induces DNA double-strand-breaks and activates checkpoints to arrest cells in G_1 and G_2.[2,34] Hundreds of cell-cycle-regulated genes were observed to change in response to DNA damage.[9,16,35,36] Genes that were not cell-cycle- regulated were easy to identify as transcriptional targets because expression of these genes was not affected by the DNA damage-induced synchronization effect. However, it is impossible in these studies to distinguish genes that were changed by primary transcriptional regulation from genes changed resulting from cell synchrony caused by the checkpoint response to DNA damage. Our model was developed to address this question. The methodology used here enabled estimation of the changes of gene expression resulting from the cell synchrony effect and identification of transcriptional targets of IR whose changes in gene expression were greater than that from cell synchrony alone.

Although the G_2 checkpoint was clearly activated at 2 hr post-IR irradiation, the expression of genes that are important for the G_2/M transition, such as *CDC2* and *CCNB1*, did not show any difference between the measured and the estimated values, indicating that post-translational modifications account for the G_2 checkpoint function at this time point and changes in expression of these genes were due to accumulation of the G_2 population (Table 5, Fig. 3b). Starting at 6 hr post-IR, the time when G_1 arrest was clearly observed, the expression of some S phase genes, like *MCM2* and *MCM3*, showed greater repression than estimated, suggesting a direct transcriptional repression mechanism in G_1 arrest. Further at 24 h post-IR, the expression of many important cell cycle-regulated genes, including *CCNB1* and *2*, *CDC2*, *CDC20*, *CDC7L1*, *CDK2*, *MCM2*, *3* and *7*, *RFC4*, *TIMELESS* and *TOP2*α showed greater repression in the observed values also suggesting direct inhibition by IR in addition to the cell synchrony effects. These results suggest that expression of some cell-cycle-regulated genes is actively changed in response to DNA damage to contribute to cell cycle arrest. Many other cell-cycle-regulated genes were just down-regulated passively in response to DNA damage secondary to cell cycle arrest. The mechanisms of primary down-regulation of the target genes are still not clear. p53 has been reported to play an important role in trans-repression of cell-cycle-regulatory genes.[35,37,38] Well-known p53-responsive genes include *CDC2*, *CCNB1*, and *TOP2α*.[39–41] Despite the transcription factors E2F and NF-Y being enriched in both groups, cell cycle-dependent element (CDE) was significantly enriched in the target group and upstream stimulating factor (USF) was enriched in the non-target group. Previous analyses of *CDC2* and *CCNB1* promoters suggested that p53 interacted with NF-Y to mediate trans-repression,[42] although a subsequent study suggested that p53 trans-repressed through interaction with SP1.[43] Conversely several groups have reported that genes containing CDE/CHR in their promoters, such as *CCNB1*, *CCNB2*, *CDC2*, *TOP2A*, *RAD51*, *CENPA*, *CDC25C*, can be directly trans-repressed by IR-induced DNA damage through a p53-dependent signaling pathway.[44–46] Two independent mechanisms, direct binding or via CDE/CHR element, are involved in p53-dependent transcriptional repression of some cell cycle-regulated genes.[44] Six of the above-mentioned target genes appeared in our target gene list (Fig. 3a). The results presented here suggest that a large set of as many as 150 cell-cycle-regulated genes may be subject to p53-dependent trans-repression in response to DNA damage.

Analysis of gene ontology in the 150 potential target genes showed that although they distributed in various categories of biological process, cellular component and molecular functions, almost all of the over-represented categories were related to cell cycle regulation, DNA metabolism and cell proliferation (Table 7). Beside the post-translational modifications of checkpoint sensors, transducers, mediators and effectors, the repression of cell cycle-regulated genes may play an important role in cell cycle checkpoint function in response to IR-induced DNA damage.

In our previous publication, 1811 IR-responding genes or ESTs were identified using the EPIG method with the same criteria for significant gene extraction.[16] Among the 1811 genes, 328 of the 406 cell cycle-regulated genes were identified, and all of the 150 IR-target genes were on the list. The other 1483 genes that were IR-responsive but not cell cycle-regulated included early DNA damage response genes, such as *CDKN1A*, *BTG2*, *GADD45A*, *PLK2*, *PLK3* and *PPMD1* that initiate or regulate cell cycle checkpoint functions. Such genes may work together with targeted repression in transcription of cell cycle-regulated genes to cause and maintain cell cycle arrest, and with genes passively responding to G_0-like growth quiescence.[16]

Identification of transcriptional targets of the DNA damage response helps us understand the mechanisms of cell cycle arrest caused by direct regulation of cell cycle-regulated genes at the level of transcription, in addition to those checkpoint functions regulated by post-translational modification of protein. Both responses appear to play important roles in maintaining cell cycle arrest. By accounting for the changes in gene expression that are indirect manifestations of cell

synchronization, this model may improve elucidation of the mechanisms of genotoxicity by environmental chemicals or therapeutic drugs that directly induce or repress transcription of target genes.

Supplementary Material

Refer to Web version on PubMed Central for supplementary material.

Acknowledgements

Supported by PHS grants ES11391, N01-ES-25497, and ES10126. We thank George Wu, Dong Xiang and Dr. Leping Li for help with microarray data analysis. We acknowledge PHS's contribution of the Software EASE used in our data analysis.

References

1. van der Meijden CM, Lapointe DS, Luong MX, Peric-Hupkes D, Cho B, Stein JL, van Wijnen AJ, Stein GS. Gene profiling of cell cycle progression through S-phase reveals sequential expression of genes required for DNA replication and nucleosome assembly. Cancer Res 2002;62:3233–43. [PubMed: 12036939]
2. Abraham RT. Cell cycle checkpoint signaling through the ATM and ATR kinases. Genes Dev 2001;15:2177–96. [PubMed: 11544175]
3. Cho RJ, Huang M, Campbell MJ, Dong H, Steinmetz L, Sapinoso L, Hampton G, Elledge SJ, Davis RW, Lockhart DJ. Transcriptional regulation and function during the human cell cycle. Nat Genet 2001;27:48–54. [PubMed: 11137997]
4. Nuwaysir EF, Bittner M, Trent J, Barrett JC, Afshari CA. Microarrays and toxicology: The advent of toxicogenomics. Mol Carcinog 1999;24:153–9. [PubMed: 10204799]
5. Waters MD, Olden K, Tennant RW. Toxicogenomic approach for assessing toxicant-related disease. Mutat Res 2003;544:415–24. [PubMed: 14644344]
6. Melo J, Toczyski D. A unified view of the DNA-damage checkpoint. Curr Opin Cell Biol 2002;14:237–45. [PubMed: 11891124]
7. Kaufmann WK, Paules RS. DNA damage and cell cycle checkpoints. Faseb J 1996;10:238–47. [PubMed: 8641557]
8. Jen KY, Cheung VG. Transcriptional response of lymphoblastoid cells to ionizing radiation. Genome Res 2003;13:2092–100. [PubMed: 12915489]
9. Tusher VG, Tibshirani R, Chu G. Significance analysis of microarrays applied to the ionizing radiation response. Proc Natl Acad Sci USA 2001;98:5116–21. [PubMed: 11309499]
10. Cho RJ, Campbell MJ, Winzeler EA, Steinmetz L, Conway A, Wodicka L, Wolfsberg TG, Gabrielian AE, Landsman D, Lockhart DJ, Davis RW. A genome-wide transcriptional analysis of the mitotic cell cycle. Mol Cell 1998;2:65–73. [PubMed: 9702192]
11. Ishida S, Huang E, Zuzan H, Spang R, Leone G, West M, Nevins JR. Role for E2F in control of both DNA replication and mitotic functions as revealed from DNA microarray analysis. Mol Cell Biol 2001;21:4684–99. [PubMed: 11416145]
12. Iyer VR, Eisen MB, Ross DT, Schuler G, Moore T, Lee JC, Trent JM, Staudt LM, Hudson J Jr, Boguski MS, Lashkari D, Shalon D, Botstein D, Brown PO. The transcriptional program in the response of human fibroblasts to serum. Science 1999;283:83–7. [PubMed: 9872747]
13. Ren B, Cam H, Takahashi Y, Volkert T, Terragni J, Young RA, Dynlacht BD. E2F integrates cell cycle progression with DNA repair, replication, and G_2/M checkpoints. Genes Dev 2002;16:245–56. [PubMed: 11799067]
14. Shedden K, Cooper S. Analysis of cell-cycle -specific gene expression in human cells as determined by microarrays and double-thymidine block synchronization. Proc Natl Acad Sci USA 2002;99:4379–84. [PubMed: 11904377]
15. Whitfield ML, Sherlock G, Saldanha AJ, Murray JI, Ball CA, Alexander KE, Matese JC, Perou CM, Hurt MM, Brown PO, Botstein D. Identification of genes periodically expressed in the human cell cycle and their expression in tumors. Mol Biol Cell 2002;13:1977–2000. [PubMed: 12058064]

16. Zhou T, Chou JW, Simpson DA, Zhou Y, Mullen TE, Medeiros M, Bushel PR, Paules RS, Yang X, Hurban P, Lobenhofer EK, Kaufmann WK. Profiles of global gene expression in ionizing-radiation-damaged human diploid fibroblasts reveal synchronization behind the G_1 checkpoint in a G_0-like state of quiescence. Environ Health Perspect 2006;114:553–9. [PubMed: 16581545]

17. Maher VM, Heflich RH, McCormick JJ. Repair of DNA damage induced in human fibro-blasts by N-substituted aryl compounds. Natl Cancer Inst Monogr 1981:217–22. [PubMed: 7341979]

18. Heffernan TP, Simpson DA, Frank AR, Heinloth AN, Paules RS, Cordeiro-Stone M, Kaufmann WK. An ATR- and Chk1-dependent S checkpoint inhibits replicon initiation following UVC-induced DNA damage. Mol Cell Biol 2002;22:8552–61. [PubMed: 12446774]

19. Deming PB, Cistulli CA, Zhao H, Graves PR, Piwnica-Worms H, Paules RS, Downes CS, Kaufmann WK. The human decatenation checkpoint. Proc Natl Acad Sci USA 2001;98:12044–9. [PubMed: 11593014]

20. Kastan MB, Onyekwere O, Sidransky D, Vogelstein B, Craig RW. Participation of p53 protein in the cellular response to DNA damage. Cancer Res 1991;51:6304–11. [PubMed: 1933891]

21. Kaufmann WK, Schwartz JL, Hurt JC, Byrd LL, Galloway DA, Levedakou E, Paules RS. Inactivation of G_2 checkpoint function and chromosomal destabilization are linked in human fibroblasts expressing human papillomavirus type 16 E6. Cell Growth Differ 1997;8:1105–14. [PubMed: 9342189]

22. Kaufmann WK, Heffernan TP, Beaulieu LM, Doherty S, Frank AR, Zhou Y, Bryant MF, Zhou T, Luche DD, Nikolaishvili-Feinberg N, Simpson DA, Cordeiro-Stone M. Caffeine and human DNA metabolism: The magic and the mystery. Mutat Res 2003;532:85–102. [PubMed: 14643431]

23. Juan G, Traganos F, James WM, Ray JM, Roberge M, Sauve DM, Anderson H, Darzynkiewicz Z. Histone H3 phosphorylation and expression of cyclins A and B1 measured in individual cells during their progression through G_2 and mitosis. Cytometry 1998;32:71–7. [PubMed: 9627219]

24. Kaufmann WK, Levedakou EN, Grady HL, Paules RS, Stein GH. Attenuation of G_2 checkpoint function precedes human cell immortalization. Cancer Res 1995;55:7–11. [PubMed: 7805043]

25. Xu B, Kim ST, Lim DS, Kastan MB. Two molecularly distinct G_2/M checkpoints are induced by ionizing irradiation. Mol Cell Biol 2002;22:1049–59. [PubMed: 11809797]

26. Unsal-Kacmaz K, Mullen TE, Kaufmann WK, Sancar A. Coupling of human circadian and cell cycles by the timeless protein. Mol Cell Biol 2005;25:3109–16. [PubMed: 15798197]

27. Cordeiro-Stone M, Boyer JC, Smith BA, Kaufmann WK. Effect of benzo[a]pyrene-diol-epoxide-I on growth of nascent DNA in synchronized human fibroblasts. Carcinogenesis 1986;7:1775–81. [PubMed: 3093114]

28. Chou JW, Paules RS, Bushel PR. Systematic variation normalization in microarray data to get gene expression comparison unbiased. Journal of Bioinformatics and Computational Biology 2005;3:225–41. [PubMed: 15852502]

29. Elkon R, Linhart C, Sharan R, Shamir R, Shiloh Y. Genome-wide in silico identification of transcriptional regulators controlling the cell cycle in human cells. Genome Res 2003;13:773–80. [PubMed: 12727897]

30. Matys V, Fricke E, Geffers R, Gossling E, Haubrock M, Hehl R, Hornischer K, Karas D, Kel AE, Kel-Margoulis OV, Kloos DU, Land S, Lewicki-Potapov B, Michael H, Munch R, Reuter I, Rotert S, Saxel H, Scheer M, Thiele S, Wingender E. TRANSFAC: Transcriptional regulation, from patterns to profiles. Nucleic Acids Research 2003;31:374–8. [PubMed: 12520026]

31. Birney E, Andrews TD, Bevan P, Caccamo M, Chen Y, Clarke L, Coates G, Cuff J, Curwen V, Cutts T, Down T, Eyras E, Fernandez-Suarez XM, Gane P, Gibbins B, Gilbert J, Hammond M, Hotz HR, Iyer V, Jekosch K, Kahari A, Kasprzyk A, Keefe D, Keenan S, Lehvaslaiho H, McVicker G, Melsopp C, Meidl P, Mongin E, Pettett R, Potter S, Proctor G, Rae M, Searle S, Slater G, Smedley D, Smith J, Spooner W, Stabenau A, Stalker J, Storey R, Ureta-Vidal A, Woodwark KC, Cameron G, Durbin R, Cox A, Hubbard T, Clamp M. An overview of Ensembl. Genome Res 2004;14:925–8. [PubMed: 15078858]

32. Russell L, Forsdyke DR. A human putative lymphocyte G_0/G_1 switch gene containing a CpG-rich island encodes a small basic protein with the potential to be phosphorylated. DNA Cell Biol 1991;10:581–91. [PubMed: 1930693]

33. Agarwal ML, Agarwal A, Taylor WR, Stark GR. p53 controls both the G_2/M and the G_1 cell cycle checkpoints and mediates reversible growth arrest in human fibroblasts. Proc Natl Acad Sci USA 1995;92:8493–7. [PubMed: 7667317]
34. Iliakis G, Wang Y, Guan J, Wang H. DNA damage checkpoint control in cells exposed to ionizing radiation. Oncogene 2003;22:5834–47. [PubMed: 12947390]
35. Burns TF, El-Deiry WS. Microarray analysis of *p53* target gene expression patterns in the spleen and thymus in response to ionizing radiation. Cancer Biol Ther 2003;2:431–43. [PubMed: 14508117]
36. Amundson SA, Bittner M, Meltzer P, Trent J, Fornace AJ Jr. Induction of gene expression as a monitor of exposure to ionizing radiation. Radiat Res 2001;156:657–61. [PubMed: 11604088]
37. Sax JK, El-Deiry WS. p53 downstream targets and chemosensitivity. Cell Death Differ 2003;10:413–7. [PubMed: 12719718]
38. Mirza A, Wu Q, Wang L, McClanahan T, Bishop WR, Gheyas F, Ding W, Hutchins B, Hockenberry T, Kirschmeier P, Greene JR, Liu S. Global transcriptional program of *p53* target genes during the process of apoptosis and cell cycle progression. Oncogene 2003;22:3645–54. [PubMed: 12789273]
39. Taylor WR, DePrimo SE, Agarwal A, Agarwal ML, Schonthal AH, Katula KS, Stark GR. Mechanisms of G_2 arrest in response to overexpression of p53. Mol Biol Cell 1999;10:3607–22. [PubMed: 10564259]
40. Taylor WR, Stark GR. Regulation of the G_2/M transition by *p53*. Oncogene 2001;20:1803–15. [PubMed: 11313928]
41. de Toledo SM, Azzam EI, Keng P, Laffrenier S, Little JB. Regulation by ionizing radiation of CDC2, cyclin A, cyclin B, thymidine kinase, topoisomerase IIalpha, and RAD51 expression in normal human diploid fibroblasts is dependent on p53/p21Waf1. Cell Growth Differ 1998;9:887–96. [PubMed: 9831241]
42. Manni I, Mazzaro G, Gurtner A, Mantovani R, Haugwitz U, Krause K, Engeland K, Sacchi A, Soddu S, Piaggio G. NF-Y mediates the transcriptional inhibition of the cyclin B1, cyclin B2, and cdc25C promoters upon induced G_2 arrest. J Biol Chem 2001;276:5570–6. [PubMed: 11096075]
43. Innocente SA, Lee JM. p53 is a NF-Y- and p21-independent, Sp1-dependent repressor of cyclin B1 transcription. FEBS Lett 2005;579:1001–7. [PubMed: 15710382]
44. St Clair S, Giono L, Varmeh-Ziaie S, Resnick-Silverman L, Liu WJ, Padi A, Dastidar J, DaCosta A, Mattia M, Manfredi JJ. DNA damage-induced downregulation of Cdc25C is mediated by p53 via two independent mechanisms: One involves direct binding to the cdc25C promoter. Mol Cell 2004;16:725–36. [PubMed: 15574328]
45. Badie C, Itzhaki JE, Sullivan MJ, Carpenter AJ, Porter AC. Repression of *CDK1* and other genes with CDE and CHR promoter elements during DNA damage-induced G_2/M arrest in human cells. Mol Cell Biol 2000;20:2358–66. [PubMed: 10713160]
46. Lange-zu Dohna C, Brandeis M, Berr F, Mossner J, Engeland K. A CDE/CHR tandem element regulates cell cycle-dependent repression of cyclin B2 transcription. FEBS Lett 2000;484:77–81. [PubMed: 11068036]

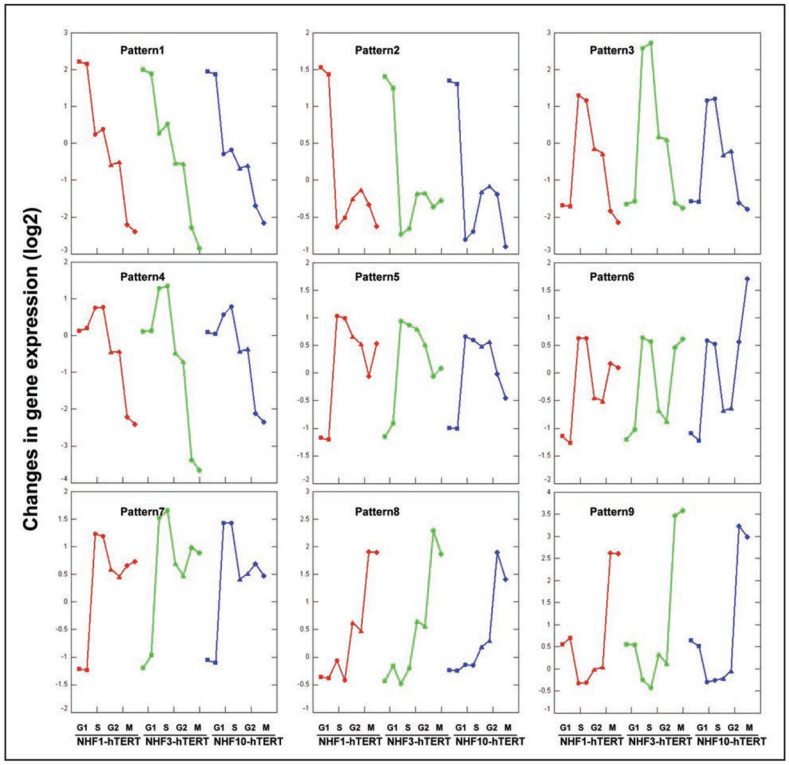

Figure 1.

Patterns of cell cycle-specific gene expression that were extracted using the EPIG method in three immortalized normal human fibroblast cell lines, NHF1, NHF3 and NHF10. Gene expression level is presented as log2 ratio of sample RNA against global reference RNA. Patterns 1 and 2 include over 500 genes that were highly expressed in G_1 phase but expressed at relatively low levels in other cell phases; Patterns 3 through 7 include over 1100 genes whose expression level was highest in S phase and lowest in G_1 or M phases; Patterns 8 and 9 included over 700 genes with maximal expression in M.

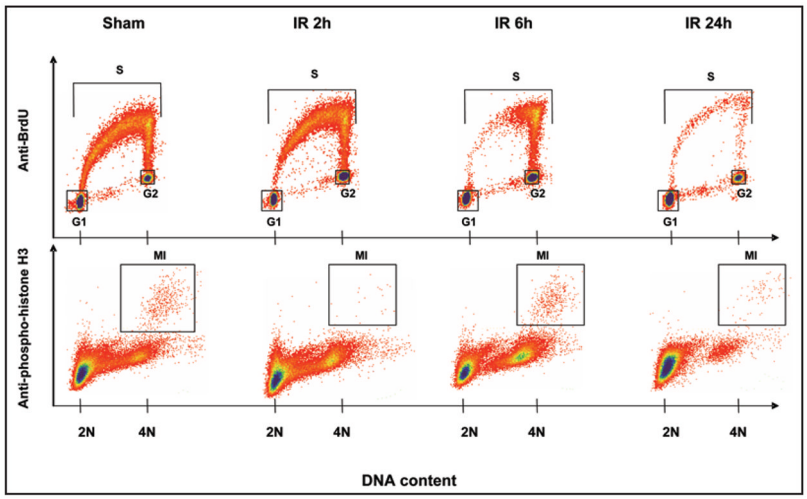

Figure 2.

Dynamic changes in cell cycle compartments at 2, 6 and 24 hr post-IR. Status of DNA synthesis through the cell cycle was determined by BrdU incorporation. S represents S phase cell population, G_1 represents G_1 phase cell population and G_2 represents G_2 phase cell population (upper panels); Mitosis was determined by anti-phospho-histone H3 antibody. MI is mitotic index that represents mitotic cell number (lower panels).

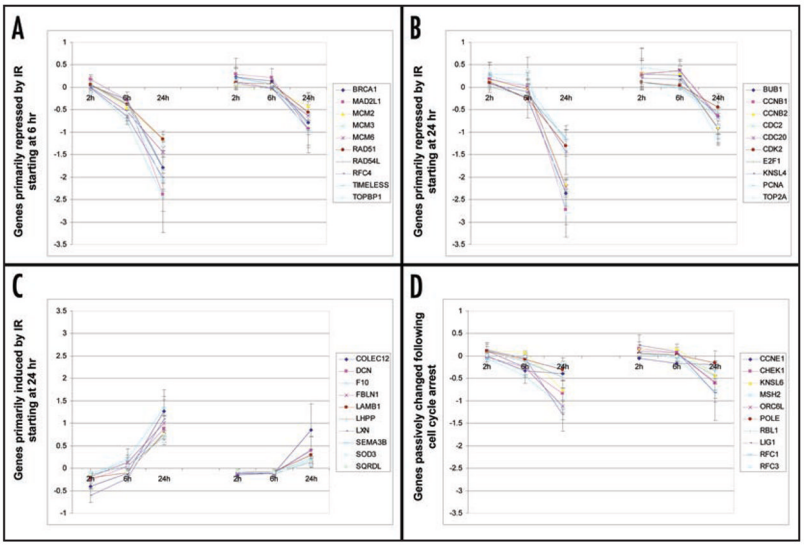

Figure 3.

Comparison of changes in expression level of selected target and non-target genes post IR-irradiation. Actual changes in cell cycle-regulated genes post IR-irradiation were measured by microarray (left), effects of cell synchronization on cell cycle-regulated genes were calculated according to changes in cell cycle compartments (right). a shows target genes that were directly trans-repressed by IR at early (6 hr) and late (24 hr) time points, b shows target genes that were directly trans-repressed by IR at only late (24 hr) time point, c shows target genes that were directly trans-induced by IR at late (24 hr) time point, d shows non-target genes whose actual changes in expression levels were very close to those from effects of cell synchronization by IR. The values depicted for each gene expression are the mean of three cell lines. Error bars indicate SE.

Table 1

Synchronization of three normal human diploid fibroblast lines (%)

Cell Line	Synchronization	G1	S	G2	M
NHF1	G1	91.0	4.5	4.4	0.2
	S	32.0	65.8	2.1	<0.1
	G2	21.1	16.5	62.0	0.3
	M	15.5	25.4	35.6	23.5
NHF3	G1	81.7	1.6	16.5	0.2
	S	23.0	71.1	5.8	0.1
	G2	16.5	10.1	70.2	3.2
	M	16.2	25.6	26.0	32.2
NHF10	G1	89.8	1.5	8.5	0.3
	S	47.0	45.8	7.1	0.1
	G2	37.7	7.1	54.4	0.9
	M	37.4	10.8	29.1	22.7

Table 2

Comparison of expression levels of cell-cycle-regulated genes before and after phase correction in NHF1-hTERT fibroblasts*

GeneBank	Sequence Name(s)	Before correction				After correction			
		G1	S	G2	M	G1	S	G2	M
AF160876	ASK	−1.84	−1.69	−0.22	−0.04	*−1.98*	*−1.63*	*0.75*	*1.74*
AF046078	BUB1	−3.18	−1.29	−0.27	0.25	*−3.53*	*−0.26*	*0.83*	*2.42*
AF053306	BUB1B	−2.25	−1.06	0.04	0.42	*−2.51*	*−0.42*	*1.02*	*2.35*
X51688	CCNA2	−1.36	−0.36	0.58	0.90	*−1.58*	*0.18*	*1.42*	*2.54*
BC006510	CCNB1	−1.89	−0.81	0.66	1.29	*−2.16*	*−0.24*	*1.84*	*4.37*
AL080146	CCNB2	−2.18	−0.56	0.21	0.58	*−2.47*	*0.32*	*1.09*	*2.11*
BC035498	CCNE1	−0.62	0.37	−0.74	−0.94	*−0.67*	*0.92*	*−1.19*	*−2.77*
AF091433	CCNE2	−1.74	−0.84	−0.92	−0.67	*−1.86*	*−0.34*	*−0.75*	*−0.10*
BC000196	CCNG1	−1.36	−2.18	−0.89	−0.76	*−1.35*	*−2.65*	*−0.27*	*0.93*
NM_004354	CCNG2	−1.56	−1.56	−0.43	−0.76	*−1.65*	*−1.57*	*0.28*	*−0.89*
BC014563	CDC2	−2.32	−0.47	0.64	0.58	*−2.67*	*0.52*	*1.80*	*0.95*
BC000624	CDC20	−1.36	−0.06	1.23	1.48	*−1.64*	*0.63*	*2.35*	*3.11*
BC019089	CDC25C	−1.47	−0.62	−0.17	0.14	*−1.63*	*−0.16*	*0.32*	*1.35*
AF081535	CDC45L	−2.32	−0.22	−0.62	−0.86	*−2.58*	*0.94*	*−0.36*	*−2.44*
BC001568	CDC5L	−0.38	−0.51	−0.20	−0.17	*−0.38*	*−0.59*	*−0.04*	*0.23*
U77949	CDC6	−3.06	0.78	−0.60	−0.51	*−3.47*	*2.90*	*−0.54*	*−2.22*
AF015592	CDC7L1	−1.84	−0.92	−1.12	−1.15	*−1.95*	*−0.41*	*−1.03*	*−1.62*
NM_005225	E2F1	−0.64	0.79	0.33	0.26	*−0.80*	*1.58*	*0.39*	*−0.66*
NM_005552	KNS2	0.61	0.62	0.83	0.97	*0.59*	*0.63*	*0.96*	*1.60*
U37426	KNSL1	−1.64	0.23	1.01	1.11	*−1.97*	*1.24*	*1.97*	*1.70*
NM_007317	KNSL4	−2.32	−0.58	−0.15	−0.17	*−2.60*	*0.37*	*0.54*	*−0.23*
NM_138555	KNSL5	−0.84	0.29	1.18	1.52	*−1.07*	*0.89*	*2.02*	*3.13*
BC014924	KNSL6	−1.56	−0.71	−0.07	0.21	*−1.73*	*−0.26*	*0.53*	*1.53*
AB035898	KNSL7	−1.64	−0.38	−0.06	−0.20	*−1.84*	*0.31*	*0.45*	*−0.67*
NM_004526	MCM2	−1.43	−0.15	−0.69	−0.79	*−1.57*	*0.55*	*−0.72*	*−1.83*
D38073	MCM3	−2.74	−0.89	−1.47	−1.09	*−2.95*	*0.13*	*−1.40*	*−0.71*
BC000142	MCM5	−1.84	−0.18	−0.51	−0.47	*−2.04*	*0.72*	*−0.32*	*−0.97*
D84557	MCM6	−2.12	−0.30	−0.76	−0.71	*−2.33*	*0.69*	*−0.61*	*−1.32*
NM_005916	MCM7	−2.74	−1.22	−1.15	−1.18	*−2.95*	*−0.39*	*−0.74*	*−1.56*
BC021566	MSH2	−2.25	0.29	−0.74	−0.71	*−2.52*	*1.69*	*−0.77*	*−2.04*
U28946	MSH6	−0.94	−0.22	−0.86	−0.22	*−1.00*	*0.19*	*−1.11*	*1.21*
BC000491	PCNA	−2.32	−0.56	−0.76	−0.67	*−2.55*	*0.41*	*−0.46*	*−0.90*
BC002369	PLK	−0.40	−0.27	0.29	0.50	*−0.46*	*−0.21*	*0.67*	*1.63*
BC001347	POLA2	−1.43	0.70	−0.06	−0.01	*−1.67*	*1.87*	*−0.02*	*−0.96*
D29013	POLB	−1.03	−0.54	−0.17	−0.30	*−1.13*	*−0.27*	*0.19*	*−0.54*
M80397	POLD1	−2.47	−0.86	−1.25	−1.22	*−2.66*	*0.02*	*−1.11*	*−1.77*
M87338	RFC2	−1.09	−0.29	−0.43	−0.60	*−1.19*	*0.15*	*−0.33*	*−1.44*
BC024022	RFC4	−2.56	−0.07	−0.74	−0.43	*−2.85*	*1.29*	*−0.56*	*−0.52*
BC001866	RFC5	−2.00	0.06	−0.30	−0.42	*−2.25*	*1.18*	*−0.03*	*−1.52*
AK027851	SNK	−1.56	−0.71	−0.69	−0.71	*−1.67*	*−0.25*	*−0.47*	*−0.95*
J04088	TOP2A	−2.74	−2.06	0.11	0.08	*−3.01*	*−1.72*	*1.65*	*1.69*
NM_006001	TUBA2	−0.34	−0.01	0.10	0.06	*−0.39*	*0.16*	*0.25*	*−0.05*
NM_025019	TUBA4	−0.49	0.52	0.68	0.31	*−0.64*	*1.06*	*1.03*	*−0.98*
BC019829	TUBB2	0.01	0.18	−0.07	0.06	*0.01*	*0.27*	*−0.20*	*0.24*
BC000748	TUBB4	−0.22	0.86	0.80	0.15	*−0.35*	*1.44*	*1.04*	*−2.26*

* The expression levels in this and following tables were presented as log2 transformed ratios of our sample RNA against global reference RNA.

Table 3

Gene number and selected genes in each expression cycle-phase-specific pattern

Patterns	No.*	Selected Genes**
Pattern 1	236 (39)	CASP1, CCRK, G0S2, SOX4, HMOX1, SUI1, TOP1MT
Pattern 2	287 (25)	CREM, EEF2, EIF4A2, GFPT2, IL6, MYC, SOD2
Pattern 3	473 (95)	ATR, CDC45L, CDC6, CDC7L1, CDKN2D, E2F1, EXO1, FANCA, FANCG, MCM2, MCM5, MCM6, MSH2, POLA2, RFC2, RFC5, SNK (PLK2), TIMELESS, TUBA4, XRCC1, XRCC5,
Pattern 4	212 (15)	ALDH1A3, CNK, DUSP6, EGR2, NCOR2, PIG8, CCNE1
Pattern 5	79 (16)	CCNG2, H1F2, PIG3, RAD50
Pattern 6	19 (2)	RFC4, RFC1
Pattern 7	358 (156)	BARD1, BLM, BRCA1, BUB1, CCNB2, CDC2, CDCA1, CDK2, CDKN2C, CDKN3, CHEK1, DDB2, MCM3, MCM7, ORC3L, ORC4L, ORC6L, PCNA, PLAB, POLB, POLE, RAD1, RAD51, RAD54B, RAD54L, RFC3, SMC2L1, SOD1, TOP2A, TOPK, WEE1
Pattern 8	302 (45)	ASK, BUB1B, CCNA2, CCNB1, CDC20, CDC25C, CDC27, CENPA, CENPE, PLK, POLG2, RAD21
Pattern 9	444 (13)	BAG3, BAG4, BNIP2, CDC2L5, CDK7, EIF5, HSPA1A, HSPA1L, HSPA8, ID3, TP53BP2
Total	2410 (406)	

* Numbers of cell cycle-regulated genes confirmed in normal cycling cell population are presented in the parentheses.

** The list and expression levels through cell cycle phases of the 406 cell-cycle-regulated genes are provided as Supplementary (Table 8).

Table 4

The proportions of cell cycle compartments in seven sham-treated NHF1 cells

	G1	S	G2	M
sham1	48.9	39.4	10.3	1.5
sham2	52.7	35.7	9.7	1.9
sham3	71.4	20.8	6.3	1.5
sham4	72.6	19.0	6.9	1.5
Sham5	73.1	19.6	5.9	1.4
Sham6	77.9	15.4	5.5	1.1
Sham7	83.0	10.5	6.0	0.5

Table 5

Changes of cell cycle compartments after IR irradiation

Cell line	Treatment	G1	S	G2	M
NHF1	sham	49.4	39.8	10.4	1.5
	1.5 Gy 2h	48.9	36.7	15.1	0.1
	1.5 Gy 6h	44.2	30.9	23.4	1.5
	1.5 Gy 24h	86.4	2.2	9.9	0.2
NHF3	sham	71.0	14.5	14.1	1.2
	1.5 Gy 2h	59.8	17.2	22.5	0.2
	1.5 Gy 6h	64.5	11.2	23.8	1.5
	1.5 Gy 24h	85.8	0.6	12.7	<0.1
NHF10	sham	65.6	23.7	9.7	1.3
	1.5 Gy 2h	58.1	26.1	15.5	<0.1
	1.5 Gy 6h	61.6	16.7	20.8	1.2
	1.5 Gy 24h	84.5	1.3	12.4	0.1

Table 6

Gene ontology analysis of biological processes in 150 potential target and 163 non-target genes

	Gene Category	List Hits	List Total	Population Hits	Population Total	Bonferroni
Targets	mitotic cell cycle	41	116	290	9996	2.86×10^{-30}
	cell cycle	52	116	624	9996	1.13×10^{-28}
	DNA metabolism	41	116	444	9996	6.09×10^{-23}
	cell proliferation	55	116	953	9996	1.00×10^{-22}
	M phase	24	116	141	9996	8.29×10^{-18}
	DNA replication and chromosome cycle	24	116	162	9996	2.17×10^{-16}
	nuclear division	22	116	136	9996	1.49×10^{-15}
	mitosis	19	116	106	9996	8.26×10^{-14}
	M phase of mitotic cell cycle	19	116	108	9996	1.17×10^{-13}
	DNA replication	19	116	131	9996	4.02×10^{-12}
	S phase of mitotic cell cycle	19	116	132	9996	4.61×10^{-12}
	DNA dependent DNA replication	14	116	66	9996	2.37×10^{-10}
	DNA repair	19	116	166	9996	2.69×10^{-10}
	response to endogenous stimulus	20	116	199	9996	5.76×10^{-10}
	response to DNA damage stimulus	19	116	196	9996	4.70×10^{-09}
	regulation of cell cycle	23	116	365	9996	7.91×10^{-08}
	cell growth and/or maintenance	70	116	3129	9996	1.05×10^{-07}
	cell cycle checkpoint	9	116	34	9996	2.12×10^{-06}
	regulation of mitosis	8	116	27	9996	1.02×10^{-05}
	mitotic checkpoint	6	116	13	9996	1.38×10^{-04}
	cytokinesis	10	116	89	9996	4.72×10^{-04}
	DNA replication initiation	6	116	17	9996	6.38×10^{-04}
	nucleobase\, nucleoside\,nucleotide and nucleic acid metabolism	52	116	2409	9996	8.50×10^{-04}
	obsolete biological process	16	116	409	9996	4.11×10^{-02}
	DNA binding	41	108	1756	10128	3.46×10^{-04}
	ATP binding	25	108	945	10128	2.34×10^{-02}
	adenyl nucleotide binding	25	108	956	10128	2.82×10^{-02}
Non-targets	mitotic cell cycle	24	119	290	9996	1.96×10^{-10}
	DNA replication and chromosome cycle	16	119	162	9996	4.53×10^{-07}
	cell cycle	27	119	624	9996	8.30×10^{-06}
	DNA replication	13	119	131	9996	2.95×10^{-05}
	S phase of mitotic cell cycle	13	119	132	9996	3.21×10^{-05}
	cell proliferation	29	119	953	9996	3.00×10^{-03}
	nucleotide binding	32	119	1184	10128	6.70×10^{-03}
	DNA metabolism	18	119	444	9996	1.21×10^{-02}
	nuclear division	10	119	136	9996	2.27×10^{-02}
	M phase	10	119	141	9996	3.02×10^{-02}

The list and changes in e x pression levels of the 150 target and 163 non-target genes are provided as Supplementary (Table 9).

Table 7

Comparison of transcription factors (TFs) between target and non-target genes [a]

	TF (TRAnSFAC Accnum)	No. of genes	Enrichment Factor*	P-Value
Targets (150)	NF-Y (M00287)	59	2.9	4.5×10^{-15}
	E2F (M00939)	35	4.4	5.7×10^{-12}
	CDE**	49	2.0	9.9×10^{-8}
Non-targets (163)	E2F (M00939)	36	2.9	8.7×10^{-7}
	USF (M00121)	30	2.0	3.3×10^{-5}
	NF-Y (M00775)	34	1.9	3.7×10^{-5}

* Enrichment factor: the ratio between the prevalence of the TF binding site hits in the target and the background sets.

** PWM model for the CDE element were taken from [Cell cycle-dependent regulation of the human aurora B promoter BBRC 316:930-936 (2004). Kimura M et al].

[a] Putative hits of the enriched TFs as identified by PRIMA are provided as Supplementary (Table 10).